Available online at www.CivileJournal.org

Civil Engineering Journal

Vol. 5, No. 10, October, 2019

Modification of Classical Horseshoe Spillways: Experimental Study and Design Optimization

Vahid Hasanzadeh Vayghan [a], Ali Saber [b*], Soroosh Mortazavian [c]

[a] Department of Civil Engineering, Urmia University; Urmia, West Azarbaijan, Iran.

[b] Department of Civil and Environmental Engineering and Construction, University of Nevada, Las Vegas; Las Vegas, NV 89154, USA.

[c] Department of Mechanical Engineering, University of Nevada, Las Vegas; Las Vegas, NV 89154 USA.

Received 25 May 2019; Accepted 03 August 2019

Abstract

Investigation of the hydraulic aspects of spillways is one of the important issues regarding hydraulic structures. This study presents a modified horseshoe spillway (MHS) constructed by adding a flow passage and an internal weir in the bed of a classical horseshoe spillway (CHS). This modification increased the discharge efficiency and eliminated the rooster-tail hydraulic jump in CHSs. Eighteen laboratory-scale MHSs in various geometric sizes, six various CHSs, and a rectangular weir of the same width were constructed and tested under the same flow conditions. Results showed that in terms of discharge efficiency and water head reduction, CHSs and MHSs were superior to the rectangular weir. Compared to CHSs, the increased discharge flowrate in MHSs due to the internal weirs could further reduce the water head and thus increased their overall efficiencies. Design parameters effecting spillways' discharge efficiencies were investigated based on dimensional analysis. The internal to external weir length ratio in MHSs was found to be a key design factor. To determine the optimal geometric design of CHS and MHS models, cubic polynomial models considering dimensionless parameters and their interactions were fitted to the experimental results. The cubic models revealed that higher discharge efficiencies in MHSs tended to occur at relatively low water heads and high internal to external weir lengths ratios.

Keywords: Curved Spillways; Discharge Coefficient; Dimensional Analysis; Stage-discharge Equation; Hydraulic Structures; Dam Construction.

1. Introduction

The main objective of building a spillway is to safely convey the excess flood from a reservoir to the downstream of a dam. According to the U.S. Bureau of Reclamation [1], a spillway usually consists of a control structure to control flow of water, a chute or conduit to convey water out of the reservoir, and a terminal stilling basin to dissipate the energy of water flowing downstream of the dam. The weir length in a spillway is one of the most important parameters to control the spillway's discharge capacity [2]. The flowrate in a standard weir can be calculated as [2, 3]:

$$Q = C_d L \frac{2}{3} \sqrt{2g} h^{3/2} \quad (1)$$

Where Q (m^3/s) is the discharge flow, h (m) is the water head over the spillway, g ($m^2.s^{-1}$) is the acceleration due to gravity, L (m) is the spillway crest length, and Cd is the discharge coefficient.

In the plan-view, spillways can have various shapes, including labyrinth, curved, and straight (known as rectangular weir) [4]. A labyrinth spillway is a corrugated form of a rectangular weir whose overall crest length is elongated in order

* Corresponding author: sabersic@unlv.nevada.edu

http://dx.doi.org/10.28991/cej-2019-03091396

to obtain a higher discharge efficiency [5]. Similarly, the increased crest length of curved spillways can enhance their overall discharge efficiency. Horseshoe, duckbill, and semi-circular spillways are common forms of curved spillways. Generally, when compared to standard rectangular weirs, curved and labyrinth spillways have some advantages, including increased effective length, less flow fluctuations within the intake channel, a greater flow aeration ability, and the capability to convey a greater flow rate with a smaller change in the water head over the spillway [2]. In places where topographic conditions restrict the width of the approach channel, labyrinth spillways can be employed to concentrate the discharge into a chute or narrow conveyor. This would significantly reduce the spillways' approach excavation [6,7].

In order to develop an equation for predicting the head discharge in submerged labyrinth weirs, Tullis et al. [8] investigated the dimensionless relationship of the water head over the weir to the weir's height ratio, the length magnification which is the sidewall's length to the width of a single labyrinth weir cycle, the side wall angle, and the vertical aspect ratio

Crookston [9] investigated the discharge coefficient of labyrinth spillways using physical labyrinth spillways models with sidewall angles ranging from 6º to 35º with semi-circular and quarter circular crests. Results showed that the labyrinth spillways with a semi-circle crest had higher performance when $h/p > 0.4$. Crookston and Tullis [10] tested the hydraulic performance of linear and half-round arced labyrinth weirs with 6º and 12° sidewall angles and compared their results to half-round crest horseshoe weirs. They observed a local submergence in the labyrinth weirs with increasing upstream head on the weirs. However, despite local submergence, they found that arced labyrinth weirs had higher discharge capacities than horseshoe weirs. Seamons [11] investigated the effects of upstream apex width, sidewall angle, and channel width on the discharge efficiency of labyrinth spillways. Seamons [11] tested various laboratory-scale labyrinth weirs with sidewall angles of 12° and 15° with different upstream apex widths under flow conditions of $0.1<h/p<0.8$. Results agreed with those of Crookston's study [9] on half-round trapezoidal arced labyrinth weirs with sidewall angles of 6° and 12°. Kaya et al. [12] investigated effects of geometric parameters on discharge capacity of semi-elliptical side spillways under subcritical flow conditions. They studied the effects of dimensionless length of spillway, dimensionless effective length, dimensionless height, dimensionless ellipse radius, and upstream Froude number on the discharge coefficient. Their results indicated that the discharge coefficient of a semi-ellipse spillway generally was higher than that of a classical side spillway. Tiwari and Sharma [13] used physical models to investigate hydraulic efficiencies of an ogee and a piano key weir in a laboratory flume. Their results indicated that reducing the water head over the weir enhanced the efficiency of both types of spillway. Lapotre and Lamb [14] investigated the acceleration of upstream water into horseshoe canyons and waterfalls. Their numerical experiments revealed that normal flow, the Froude number, the ratio of the flood's width relative to the lateral backwater length and the canyon's width, and the ratio of canyon's downslope length to backwater length were the key factors influencing the acceleration factor around a canyon's brink. Dabling and Tullis (2018) [3] experimentally studied the influence of approach flow angle on the hydraulic efficiency of labyrinth weirs. They investigated the head–discharge characteristics for three different approach flow angles of 0°, 15°, and 45°. Compared to an approach flow angle of 0°, they reported no decrease in discharge efficiencies for approach flow angles < 15°, but 11% decrease for an approach flow angle of 45°.

Despite merits claimed in the literature, most studies on nonlinear spillways focused on labyrinth spillways. To the best knowledge of the authors, there are only a limited number of studies conducted on horseshoe spillways [6, 10, 14] There is a lack of study particularly focused on horseshoe spillways to characterize and optimize their hydraulic behavior.

This study presents a modified version of horseshoe spillway by adding an additional flow passage and an internal weir to the classical horseshoe spillway, thereby allowing more flow of water entering the trough. Eighteen different geometric designs of laboratory-scale modified horseshoe spillways (MHSs) were constructed and tested under different flow conditions. For comparison, six various classical horseshoe spillways (CHSs) having the same sizes as MHS models, and a rectangular weir having the same width as CHS and MHS models were constructed and tested under the same flow conditions. This is the first study that investigates effects of geometric design on various hydraulic characteristics including discharge coefficient, water head, and flow profile in classical and modified horseshoe spillways. Factors affecting discharge coefficient in CHS and MHS models were determined based on dimensional analysis. Finally, cubic regression models were fitted to the experimental data, and subsequently used to determine the optimized geometric designs yielding the highest efficiencies in both CHS and MHS spillways.

2. Materials and Methods

2.1. Modification of Classical Horseshoe Spillways

In a CHS, the surplus water overflows from the right, left, and curved walls. The overflowing water in the trough then is conveyed through a chute to the downstream of the dam. Figure 1a shows a schematic CHS, and Figures 1b and 1c show the flow in a laboratory-scale CHS model built in this study. In order to improve the efficiency of the CHS, a modified version of horseshoe spillways (MHS) was constructed by introducing an opening and an internal weir into the middle of the CHS's trough (Figure 1d) to allow more flow of water entering the trough. Figures 1e and 1f show the flow in a laboratory-scale MHS model constructed in this study.

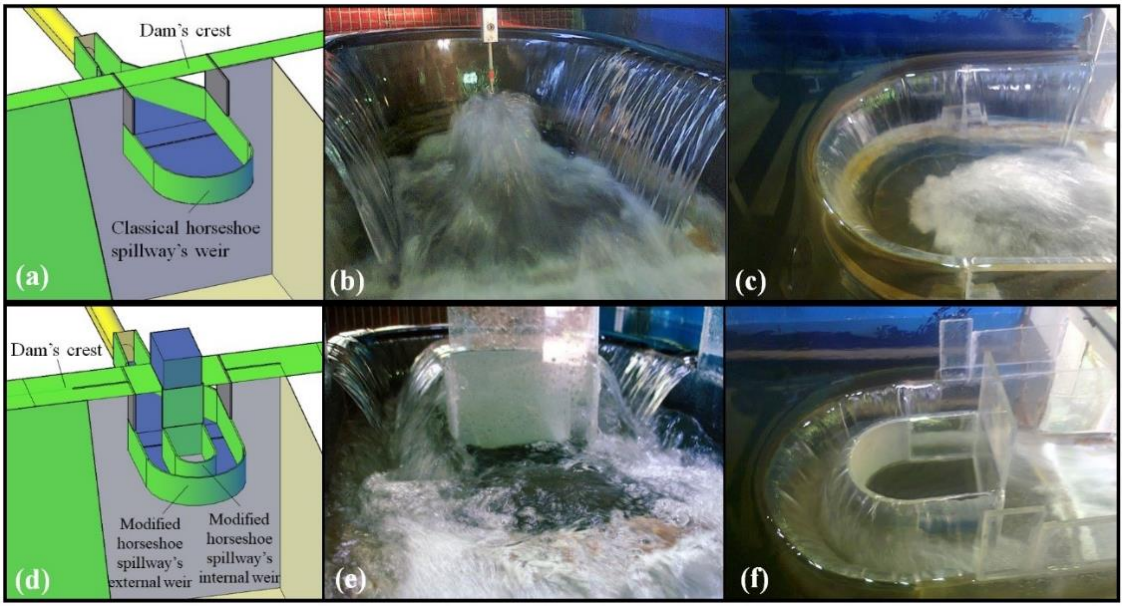

Figure 1. (a) Schematic diagram of a CHS, (b) view from the downstream and (c) view from the top of a laboratory-scale CHS model; (d) schematic diagram of an MHS, (e) view from the downstream and (f) view from the top of a laboratory-scale MHS model

2.2. Laboratory-scale Sizes of CHS, MHS, and Rectangular Spillways

In this study, six various CHS models, eighteen various MHS models, and a rectangular spillway were constructed using Plexiglas®. Sample pictures and videos of constructed CHS, MHS, and rectangular spillways could be found in the supplementary files (Figure S1 in supplementary word file and videos S1 and S2). The CHS models had various weir lengths of 76.0, 88.0, 100.0, 112.0, 124.0, and 136.0 cm. Each CHS model consisted of a semi-elliptical segment, two straight parallel walls, and a floor with a slope of 0.036. The length and semi-minor axis of the semi-elliptical segment in all CHS models were fixed at 74.0 cm and 23.0 cm, respectively. To construct six different sizes of CHS models, two parallel walls were varied in six different lengths of 1.0, 7.0, 13.0, 19.0, 25.0, and 31.0 cm, resulting in total weir lengths of 76.0, 88.0 100.0, 112.0, 124.0, and 136.0 cm. The height of the semi-elliptical wall in all CHS models at the most upstream of the spillways was 15.0 cm. Plan and section views of CHS models are shown in Figure 2a.

Geometric design of MHS models was similar as CHSs, but with an additional internal wire constructed by introducing a duct in the spillway's bed and erecting walls around it in the spillway's trough. For the internal weir lengths in MHS models, 1:2.5, 1:5, and 1:10 scales of the largest CHS model with a total weir length of 136.0 cm were constructed. These three different scales resulted in the total weir lengths of 54.4 cm, 27.2 cm, and, 13.6 cm, and semi-minor axes of 9.2 cm, 4.6 cm, and 2.3 cm, respectively, for the internal weirs in MHSs. Figure 2b shows plan and section views of MHS models. Detailed information about dimensions of different CHS and MHS models is presented in Table 1.

In addition, a straight rectangular weir with a width of 46.0 cm, the same as widths of CHS and MHS models, was also constructed and its experimental results were compared with those of the CHS and MHS models.

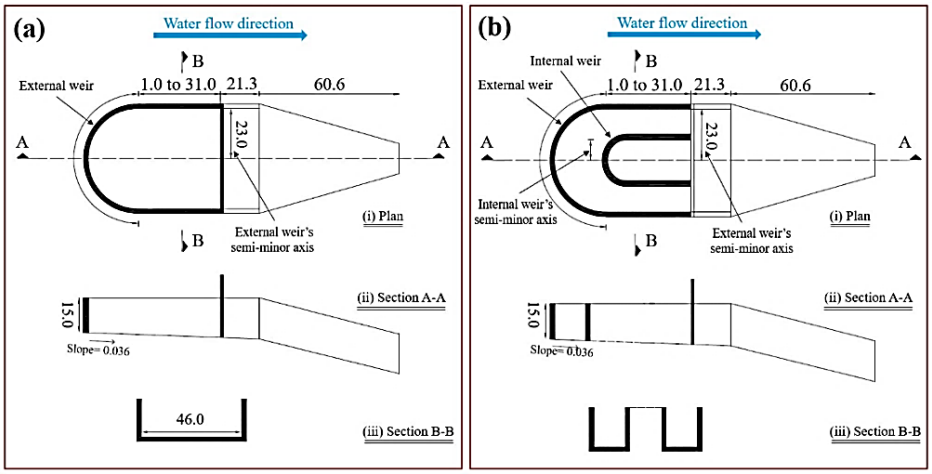

Figure 2. Plan and section views of (a) CHS, and (b) MHS models. Water flow directions from the upstream to the downstream are shown by arrows. All length numbers are in cm

Table 1. Dimensions of different constructed CHS, MHS, and rectangular weir models used in experiments

Spillway type	External weir's semi-minor axis, cm	Length of semi-elliptical segment in the external weir, cm	Total length of the external weir (Lext), cm	Internal weir's semi-minor axis, cm	Total length of the internal weir (Lint), cm
CHS	23.0	74.0	76.0, 88.0, 100.0, 112.0, 124.0, 136.0	N/A	N/A
MHS	23.0	74.0	76.0, 88.0, 100.0, 112.0, 124.0, 136.0	9.2	54.4
	23.0	74.0	76.0, 88.0, 100.0, 112.0, 124.0, 136.0	4.6	27.2
	23.0	74.0	76.0, 88.0, 100.0, 112.0, 124.0, 136.0	2.3	13.6
Rectangular	N/A	N/A	46.0	N/A	N/A

2.3. Experimental Setup

Water supply system used in this study consisted of an underground pool equipped with a pump with a maximum flowrate of 60 L.s^{-1}. The pump was used to transfer water from the underground pool to a free-surface cylindrical tank with a volume of 2.5 m^3. The cylindrical tank was equipped with an internal weir to keep water at a constant level of 3.7 m to maintain a constant water head in all experiments. An open-top rectangular cube with dimensions of 180 cm length × 100 cm width × 120 cm height was used as the main reservoir. The crest heights in both CHS and MHS were 95 cm above the reservoir's bed. In order to simulate quiescent conditions in the reservoir, a flow tranquilizer was employed at 100 cm upstream of the spillways. Figure 3a shows a schematic of the experimental setup.

The flow tranquilizer was made of two meshed-metallic frames (100 cm width × 120 cm height) with 10 cm distance in between. The distance between the frames was filled with wool fabrics and gravel with a grain size ranging from 10.0 mm to 18.0 mm. The use of a flow tranquilizer resulted in velocities of less than 6 cm.s^{-1} at spillway's crest elevation.

2.4. Experimental Measurements

The inflow water head was measured at 60.0 cm upstream of the spillways using a point gauge. Current velocity was measured with a micro-current meter. Using a point gauge with an accuracy of ±0.1 mm, flow profiles over and inside the spillways were measured every 2.0 cm along the A-A and B-B axes shown in Figure 2. The total outflow discharge from the spillways was measured using a stilling basin equipped with a calibrated triangular spillway, with an apex angle of 53º 8′ at the downstream of stilling basin (see Figure S3 in supplementary information). The relationship between the discharge flowrate and the water head overflowing the triangular weir was calculated as [15]:

$$Q = 8/15 \sqrt{2g}\, C_{de}\, tan\ \theta/2\, H_d^{2.5} \quad (2)$$

Where Q (m^3 s^{-1}) is discharge flow, g (m.s^{-2}) is gravitational acceleration, C_{de} is the discharge coefficient, θ is the apex angle of triangular weir, and H_d is the water head overflowing the triangular weir. Rating curve of the triangular weir downstream of the model is presented in Figure 3b.

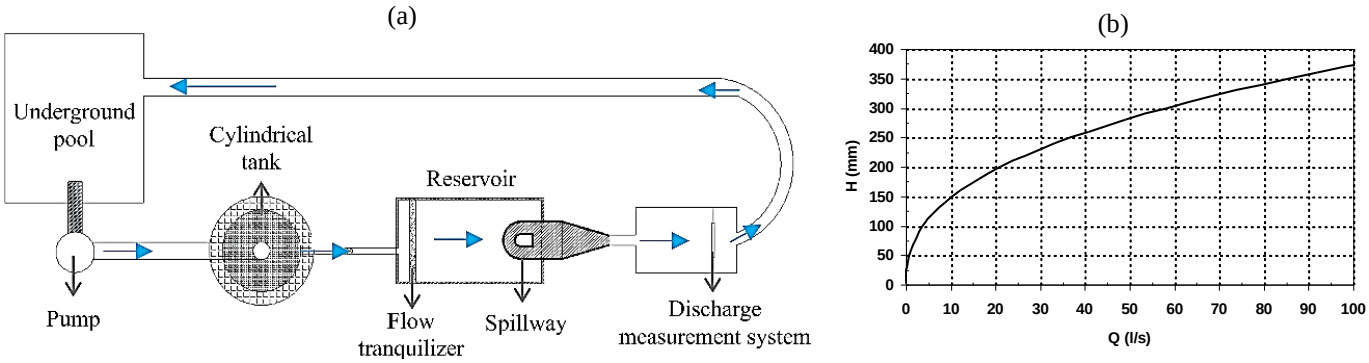

Figure 3. (a) Schematic of the experimental setup, and (b) rating curve of a triangular weir used

2.5. Experimental Design

In this study, three sets of experiments were conducted using CHS, MHS, and rectangular spillways to investigate the hydraulic efficiency of spillways under a variety of flow conditions. Table 2 describes the objectives of different experiments.

Table 2. Description of experiments for investigating hydraulic efficiency of spillways under various flow conditions

Set No.	Description	Variable parameters	Objective(s)	Number of tests
1	Experiments on CHSs	Flowrate, water head, spillway's weir length	To investigate hydraulic efficiency of CHSs	42
2	Experiments on MHSs	Flowrates in internal and external weirs, water head, internal and external weir lengths	To investigate hydraulic efficiency of MHSs	126
3	Experiments on rectangular weir	Flowrate, water head	To compare hydraulic efficiency of the rectangular weir with CHS and MHS models	7

In the first set of experiments, six different CHS models were tested under various water heads and flowrates conditions. The second set of experiments was conducted on eighteen different MHS models, and the third set of experiments was conducted on a straight rectangular weir. In all three experimental sets, hydraulic efficiency of spillways was investigated under seven different flowrates of 7.5, 8.5, 9.5, 10.5, 11.5 12.5, and 13.5 $L.s^{-1}$.

2.6. Calculation of Discharge Coefficients

Equation 1 was used to calculate the discharge coefficient through CHSs and external weirs in the MHSs. Since an MHS is a combination of a CHS (external weir) and an internal weir, the total discharge (Q) through the entire MHS consisted of discharges through the external and internal weirs, expressed as:

$$Q = Q_1 + Q_2 \quad (3)$$

Where Q_1 and Q_2 are the discharge overflowing the external and internal weirs, respectively. As mentioned, Equation 2 was used to calculate the total discharge (Q) based on the water head measured at the downstream triangular weir. To obtain stage-discharge equations for different weir lengths of CHSs (that functioned as the external weirs in MHSs), steady-state water heads above the weirs of all CHS models at various flowrates were measured. Then, by fitting a non-linear least-square regression model to the flowrate and water head (h) data points, a stage-discharge equation for each weir length was obtained. Table 3 summarizes the stage-discharge equations obtained for various CHS sizes.

Table 3. Stage-discharge equations obtained for different CHS sizes that functioned as external weirs in MHS models

Weir length (cm)	Stage-discharge equation	R^2
76.0	$Q_1 = 1.363 \times h^{1.5}$	0.979
88.0	$Q_1 = 1.657 \times h^{1.5}$	0.975
100.0	$Q_1 = 1.966 \times h^{1.5}$	0.994
112.0	$Q_1 = 2.191 \times h^{1.5}$	0.981
124.0	$Q_1 = 2.321 \times h^{1.5}$	0.968
136.0	$Q_1 = 2.622 \times h^{1.5}$	0.947

Values of Q_1 in MHS models were determined based on the stage-discharge equations obtained for CHS models of the same size. Having the values of Q from the downstream triangular weir and Q_1 values obtained from the stage-discharge equations (Table 3), discharge overflowing the internal weirs (Q_2) in MHSs were determined according to Equation 3.

The equal elevations of the internal and external weirs' walls in MHSs resulted in equal water heads (h) above both the internal and external weirs. The values of Q_2, h, and length of the internal weir were substituted into Equation 1 and the discharge coefficient for the internal weirs in MHS models were also calculated.

2.7. Dimensional Analysis of CHSs and External Weirs in MHSs

The discharge coefficient in a spillway can be described as a function of parameters affecting the flow of water in the spillway. Dimensional analysis based on π-Buckingham theorem can be employed to determine the dimensionless parameters affecting the efficiency of a spillway. Applying dimensional analysis, the discharge coefficient in CHSs, C_c, can be written as [16-19]:

$$C_c = f\left(h/p, L_{ext}/p\right) \quad (4)$$

Where, h is water head above the spillway, p is spillway's height from the reservoir's bed, L_{ext} is the spillway's weir length, and b is the width of the spillway.

Similarly, the discharge coefficient for the internal weirs in MHSs, C_{int}, can be written as [16-19]:

$$C_{int} = f\left(h/L_{ext}, h/p, h/L_{int}\right) \quad (5)$$

Where, L_{int} is internal weir length. In this study the heights of both internal and external weir walls from the reservoir's bed were the same, resulting in equal values of p for both the internal and external weirs in MHS models.

More details regarding dimensional analysis and simplifications used for deriving Equations 5 and 6 can be found in the supplementary information.

2.8. Statistical Analysis and Design Optimization of Spillways

From an economical point of view, the main objective in design of a spillway is to reduce spillway's size while still obtaining a desired discharge flowrate. Hence, the interactions between the spillway size and the water head, as well as their effects on the discharge efficiency needs to be taken into account.

In order to consider the simultaneous effects of independent dimensionless parameters and their interactions on the discharge efficiency of spillways, cubic polynomial models were fitted to the experimental results from both CHS and MHS models. A cubic model with C_c as the response (dependent variable) and h/p and L_{ext}/b as the independent variables were considered for CHSs, and a separate cubic model with C_{int} as the response (dependent variable) and h/p and L_{int}/L_{ext} as the independent variables were considered for the internal weirs in MHSs. Analysis of variance (ANOVA) was performed to ensure the statistical significance of the independent variables and their interactions in the fitted cubic models. All statistically non-significant interactions (p-value > 0.05) were excluded from the cubic models in a stepwise manner, and the subsequent reduced cubic models were used to evaluate the optimal geometric design of the spillways.

3. Results and Discussion

3.1. Flow Pattern in CHS and MHS Models

Experiments conducted on CHSs showed that a cross-sectional flow profile inside a CHS could be divided into two parts: 1) the two overflowing nappes from the sidewalls and the stream between them, and 2) water flowing between the spillway's walls and the two overflowing nappes from the side walls. Figure 4a shows that in a CHS, the stream overflowing the curved segment collided with the streams overflowing the side walls, resulting in the creation of a rooster tail jump in spillway's trough. The cross-sectional flow profile in the MHS could be divided to three parts: (1) overflowing nappes from the external and internal weirs and the stream between them, (2) flow behind the nappes of the external weir, and (3) flow behind the nappes of the internal weir (see Figure 4b).

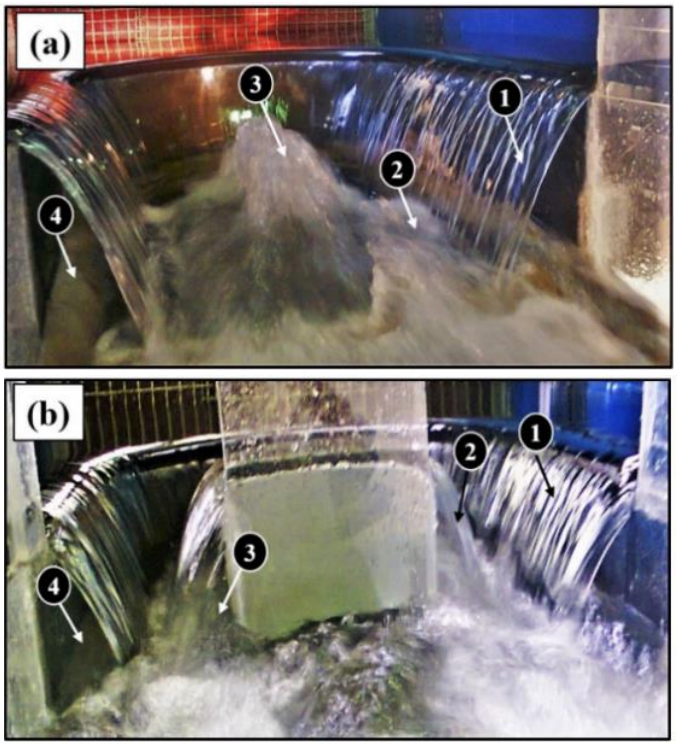

Figure 4. (a) Flow in a CHS showing: (1) overflowing nappe from the sidewall, (2) stream between the overflowing nappes, (3) rooster-tail jump, and (4) flow behind the overflowing nappe; (b) flow in an MHS showing: (1) overflowing nappe from the external weir, (2) overflowing nappe from the internal weir, (3) flow behind the overflowing nappe of the internal weir, and (4) flow behind the overflowing nappe of the external weir

Figure 5 shows the measured cross-sectional and longitudinal flow profiles in CHS and MHS models with different weir lengths at a total flowrate of 11.5 L.s^{-1}.

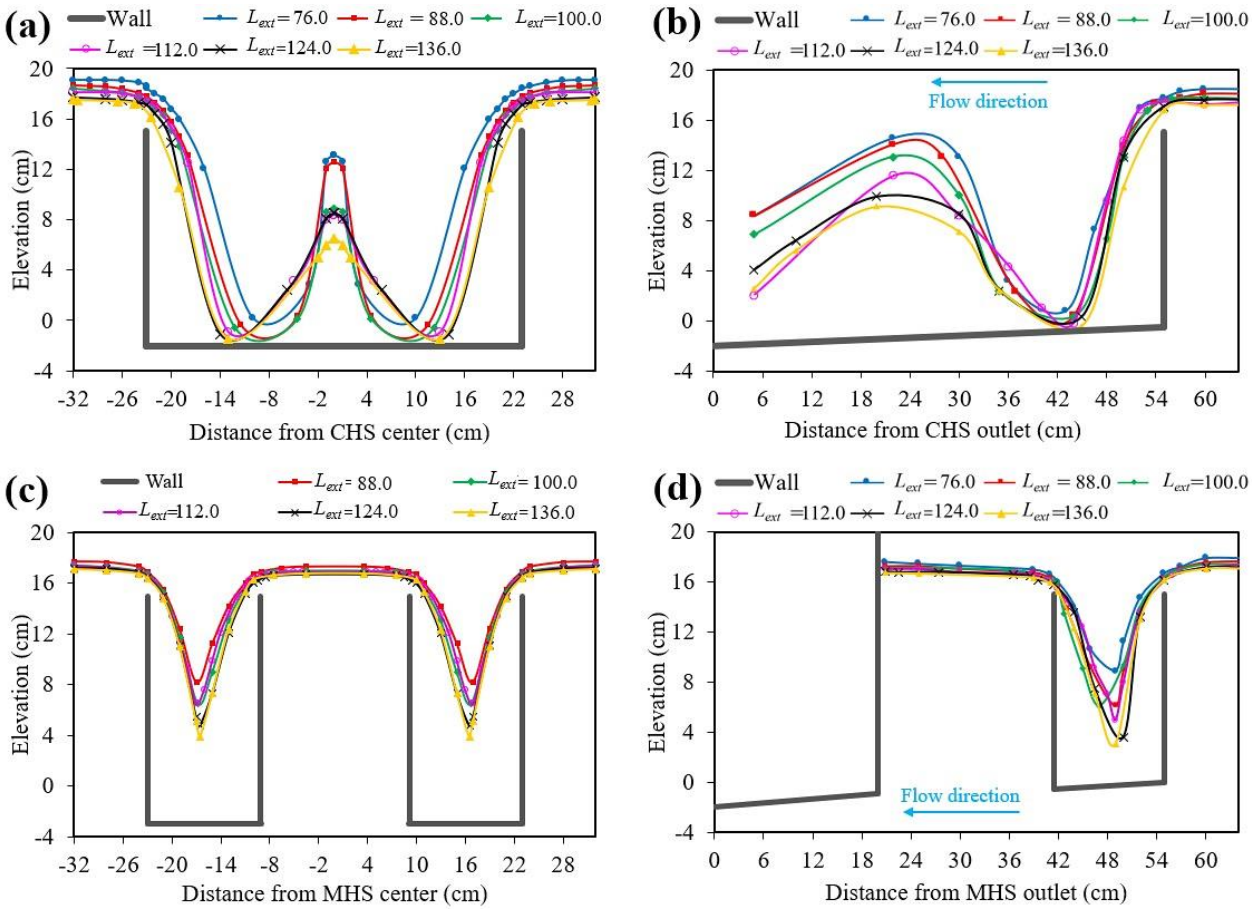

Figure 5. Cross-sectional and longitudinal profiles along A-A and B-B axes for (a, b) CHSs and (c, d), MHSs with an internal weir length of 54.4 cm (Q = 11.5 L s^{-1}, Lext values are in cm, A-A and B-B axes are shown in Figure 2)

As seen in the cross-sectional profiles of the flow in CHSs (Figures 5a and 5b) for a constant discharge, reducing the weir length increased the water head over the spillway, which subsequently resulted in an increase in the distance of the overflowing nappe from the spillway's walls. In addition, reducing the weir length increased both the height and length of the rooster-tail jump in CHSs.

For MHSs, Figures 5c and 5d show that decreasing the length of external weir (L_{ext}), increased the water level in both the cross-sectional and longitudinal profiles. Decreasing the external weir length in MHS models increased the distance between the junction of the two overflow nappes and the spillway's bed.

Comparison of the flow profiles in CHS and MHS models shows that the addition of internal weirs to a CHS could eliminate the formation of the rooster-tail jump, hence increasing the durability of the spillway's structure.

3.2. Head Reduction in CHS and MHS Models

Figure 6 shows the experimental results of water head measurements and compares the water head over CHS and MHS models with a rectangular spillway of the same width under the same flow conditions. As seen from Figure 6, significantly greater water heads occurred in the rectangular weir compared to CHS and MHS models, in all the experimented flowrates. In addition, the water heads over the MHSs were considerably lower than the heads in CHSs.

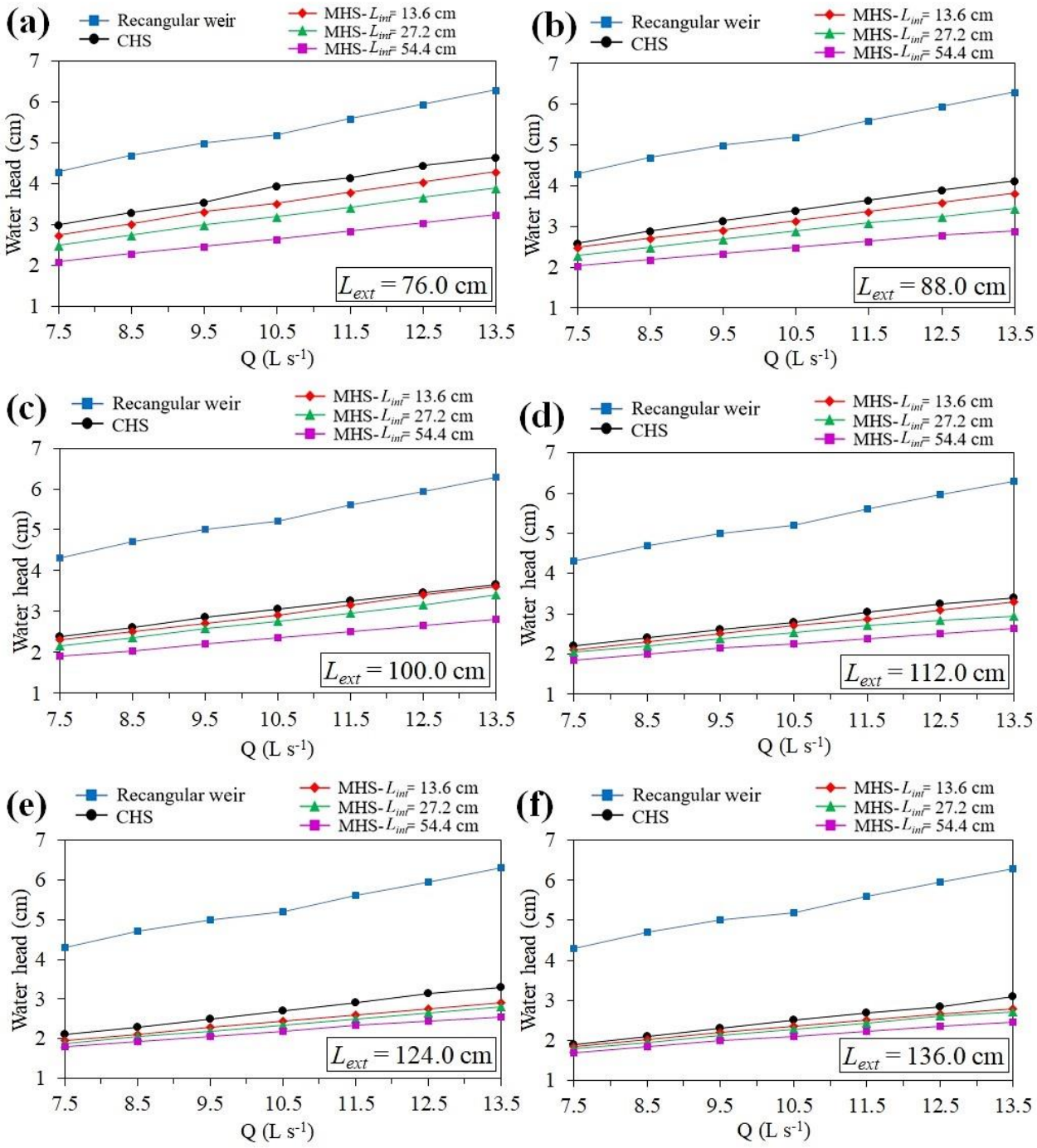

Figure 6. Water heads over MHS models with three different internal weir lengths of 13.6, 27.2, and 54.4 cm having different external weir lengths of (a) 76.0 cm, (b) 88.0 cm, (c) 100.0 cm, (d) 112.0 cm, (e) 124.0 cm, and (f) 136.0 cm, compared to water heads over CHS and a rectangular weir of the same width

As Figure 6 shows, effects of increasing the internal weir length on water head reduction in MHSs were more pronounced in spillways having smaller external weir lengths. For instance, the water head over an MHS with internal and external weir lengths of 54.4 cm and 76.0 cm, respectively, was 30% lower than a CHS of the same weir size. However, water head in an MHS with internal and external weir lengths of 54.4 and 136.0 cm was only 17% lower than for a CHS of the same external weir size. Reducing the water head in MHSs affected the fraction of water flowing through internal and external weirs. Figure 7 shows a comparative diagram of the contribution of various sizes of external weirs to the total discharge (Q) flowing through MHSs. As observed, increasing the external weir length (L_{ext}) in MHSs increased the discharge overflowing the external weirs (Q_1) and, consequently, decreased the discharge flowing through the internal weirs (Q_2). Hence, shorter length of external weirs (i.e. smaller L_{ext}) could increase the fraction of discharge flowing through the internal weirs.

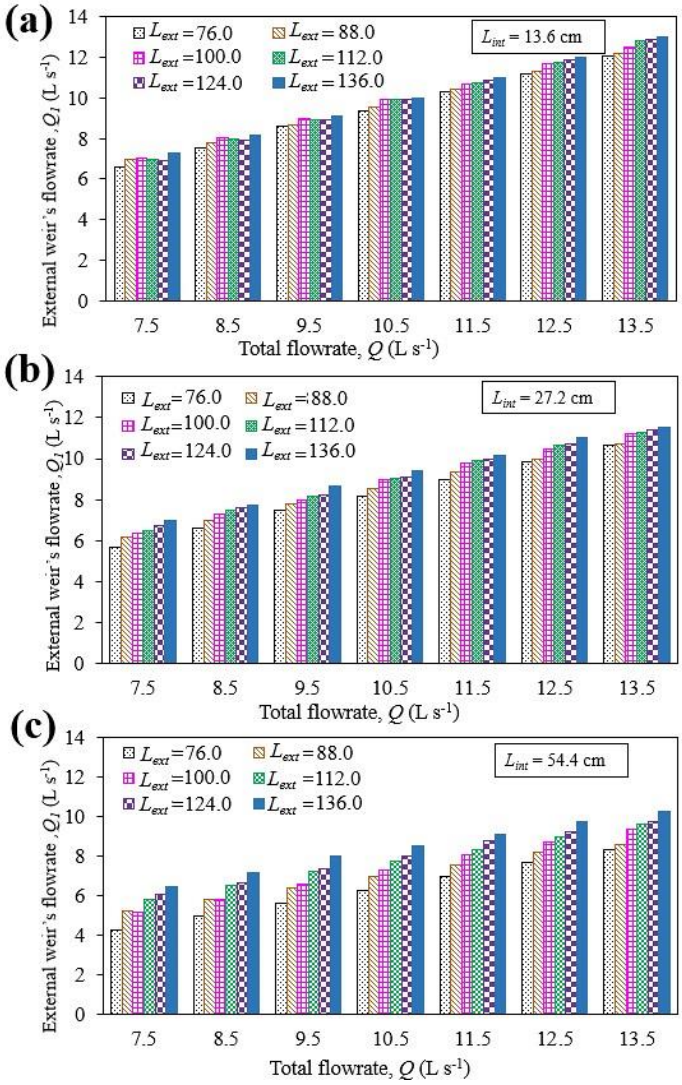

Figure 7. Contribution of various sizes of external weirs to the total discharge flowing through the MHS models with internal weir lengths of (a) 13.6 cm, (b) 27.2 cm, and (c) 54.4 cm, at different flowrates

3.3. Effects of h/p and Weir Length on the Discharge Coefficient in CHSs

Figure 8 shows the effects of the dimensionless parameter *h/p* on the discharge coefficient (C_c) in CHSs, where a constant p of 95.0 cm was used in all the experiments. As Figure 8 shows, increasing h/p in all weir lengths resulted in a linear decrease of the discharge coefficients. Characteristics of the linear regression models fitted to the experimental data obtained from CHSs with different weir lengths are listed in Table 4.

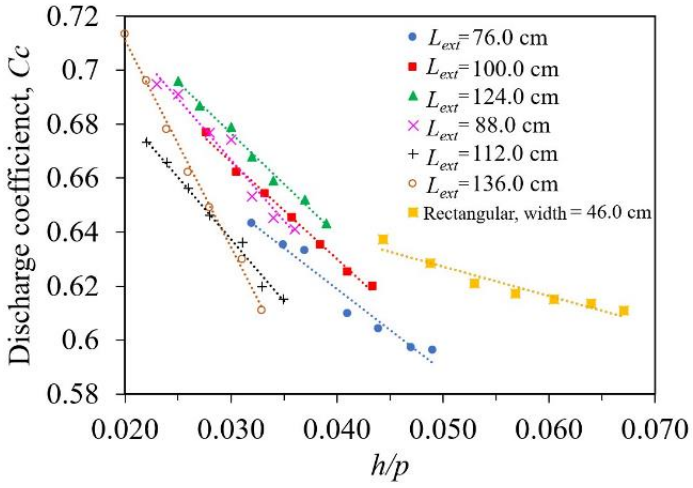

Figure 8. Variations in the discharge coefficient (Cc) versus h/p in CHSs having various external weir lengths and in a rectangular weir with a width of 46.0 cm. Dotted lines represent the fitted linear regression models

Table 4. Linear regression relationships obtained for the discharge coefficient in CHSs and rectangular weir for the dimensionless parameter h/p

Weir type	Weir length, cm	Least-squares linear regression model	R^2
Classical horseshoe spillway (CHS)	76.0	C_c= -3.0373(h/p) +0.7737	0.962
	88.0	C_c= -3.5915(h/p) +0.7737	0.992
	100.0	C_c= -3.7564(h/p) +0.7893	0.992
	112.0	C_c= -4.5418(h/p) +0.8030	0.963
	124.0	C_c= -4.6089(h/p) +0.7756	0.991
	136.0	C_c= -7.6328(h/p) +0.8633	0.996
Rectangular weir	46.0	C_{Rect} = -1.0873(h/p) +0.06816	0.927

As seen in Figure 8 and Table 4, by increasing weir length (L_{ext}) in CHSs from 76.0 to 136.0 cm, the slope of Cc versus h/p regression lines gradually decreased. Therefore, it can be concluded that CHS models with greater weir lengths could more efficiently reduce the greater water heads over the spillway. It was also shown in Figure 6 that CHSs with longer weir lengths could maintain lower water heads above their weirs. Figure 8 also shows that increasing the flowrate, in turn, increased the water head and thus decreased efficiencies of CHSs and the rectangular weir.

In the dimensionless parameter L_{ext}/b, the variable b for all the experiments was equal to a constant value of 46.0 cm; therefore, the values of Lext/b for all the experiments conducted on a specific weir length were also constant. Hence, the effects of Lext as the main variable in dimensionless parameter L_{ext}/b on discharge efficiencies at different flowrates can also be inferred from Figure 8. Hence, due to constant values of L_{ext}/b in all experiments conducted on a specific weir length, C_c versus L_{ext}/b graphs were not plotted.

3.4. Discharge Coefficient in MHSs

3.4.1. Effects of the h/Lint Ratio on the Discharge Coefficient of Internal Weirs

Figure 9 shows variation of discharge coefficient in internal weirs (C_{int}) versus h/L_{int} in MHSs with external weir lengths of 76.0, 112.0, and 136.0 cm. These three sizes were selected as the representative of short, medium, and long external weir lengths. Characteristics of the linear regression models fitted to the data points in Figure 9 (dotted lines) are listed in Table 5.

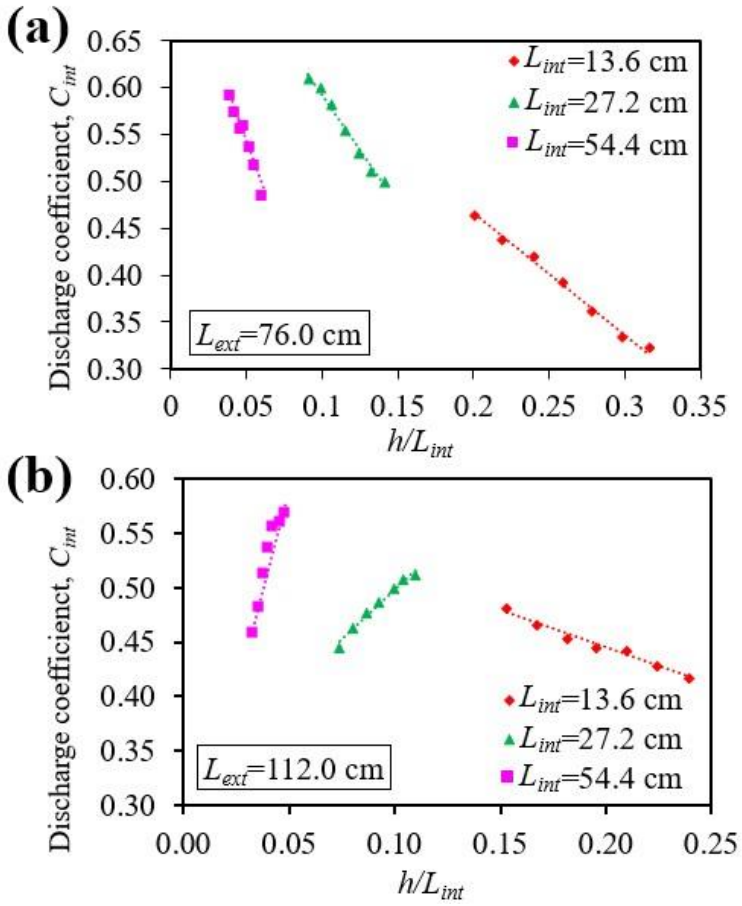

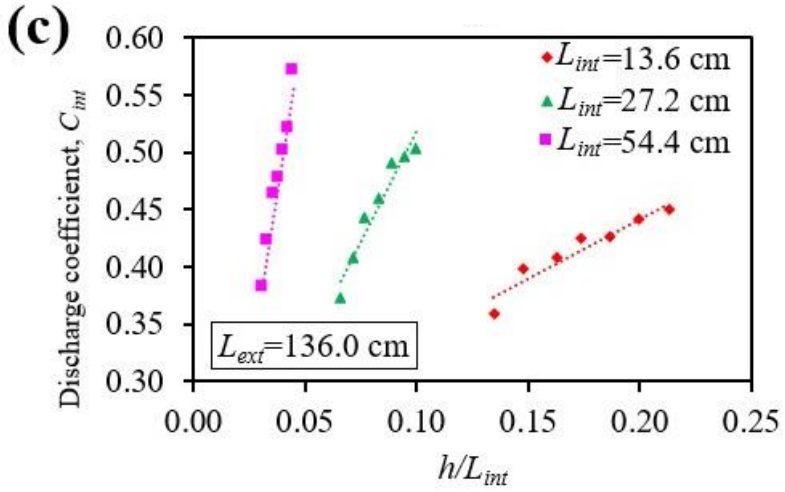

Figure 9. Variations in the discharge coefficient in the internal weirs (Cint) versus h/Lint, in MHSs with external weir lengths of (a) 76.0 cm, (b) 112.0 cm, and (c) 136.0 cm. Dotted lines represent the fitted linear regression models

Table 5. Linear regression relationships between h/Lint and the discharge coefficient in MHSs (Cint) for different lengths of internal and external weirs

External weir lengths (Lext), cm	Internal weir lengths (Lint), cm	Least-squares linear regression model	R^2
76.0	13.6	C_{int} = -1.2886(h/L_{int}) + 0.7232	0.990
	27.2	C_{int} = -2.3617(h/L_{int}) + 0.8284	0.990
	54.4	C_{int} = -2.2200(h/L_{int}) + 0.6584	0.932
112.0	13.6	C_{int} = -0.6865(h/L_{int}) + 0.5825	0.980
	27.2	C_{int} = 1.8399(h/L_{int}) - 0.3151	0.978
	54.4	C_{int} = 7.7328(h/L_{int}) + 0.9306	0.931
136.0	13.6	C_{int} = 1.0413(h/L_{int}) - 0.2340	0.915
	27.2	C_{int} = 3.8347(h/L_{int}) - 0.1355	0.946
	54.4	C_{int} = 12.2050(h/L_{int}) + 0.0080	0.973

As seen from Figure 9a, when the external weirs in MHSs were small (L_{ext} = 76.0 cm), increasing the water head over the spillway decreased the discharge efficiency of the internal weirs. This can be observed as the negative slopes for all three various sizes of the internal weirs. It could be inferred that in this situation, the internal weirs could not effectively accommodate the flowrate passing through them. Since increasing the size of the internal weirs could increase their capacities, higher efficiencies were observed as the size of the internal weirs increased (Figure 9a).

It was previously shown in Figure 7 that increasing the size of the external weirs in MHSs from 76.0 to 112.0 cm decreased the fraction of water flowing through the internal weirs. Therefore, as shown in Figure 9b for L_{ext} = 112.0 cm, a small internal weir of L_{int} = 13.6 cm still could not efficiently accommodate the fraction of water flowing through it. Hence, increasing the head resulted in bottlenecking, and thus, a decreasing trend in discharge coefficient was observed by increasing the water head over the spillway (Figure 9b, red diamonds). However, for L_{ext} = 112.0 cm, by increasing the internal weir length to 27.2 or 54.4 cm (Figure 9b, green triangles and magenta squares, respectively), the efficiency of the internal weir increased. This reflected as positive slopes, indicating that bottlenecking did not occur. Increasing the external weir length to L_{ext} = 136.0 cm (Figure 9c) could even further decrease the fraction of the flowrate passing through the internal weirs; thus, bottlenecking did not occur. Hence, by increasing the size of the internal weirs in MHS models, the positive slope of the C_{int} versus h/L_{int} also increased.

3.4.2. Effects of the h/Lext Ratio on the Discharge Coefficient of the Internal Weirs

Figure 10 shows variations in the discharge coefficient of internal weirs (C_{int}) versus h/L_{ext} in MHSs with internal weir lengths of 13.6, 27.2, and 54.4 cm. Characteristics of the linear regression models fitted to the data points in Figure 10 (dotted lines) are listed in Table 6.

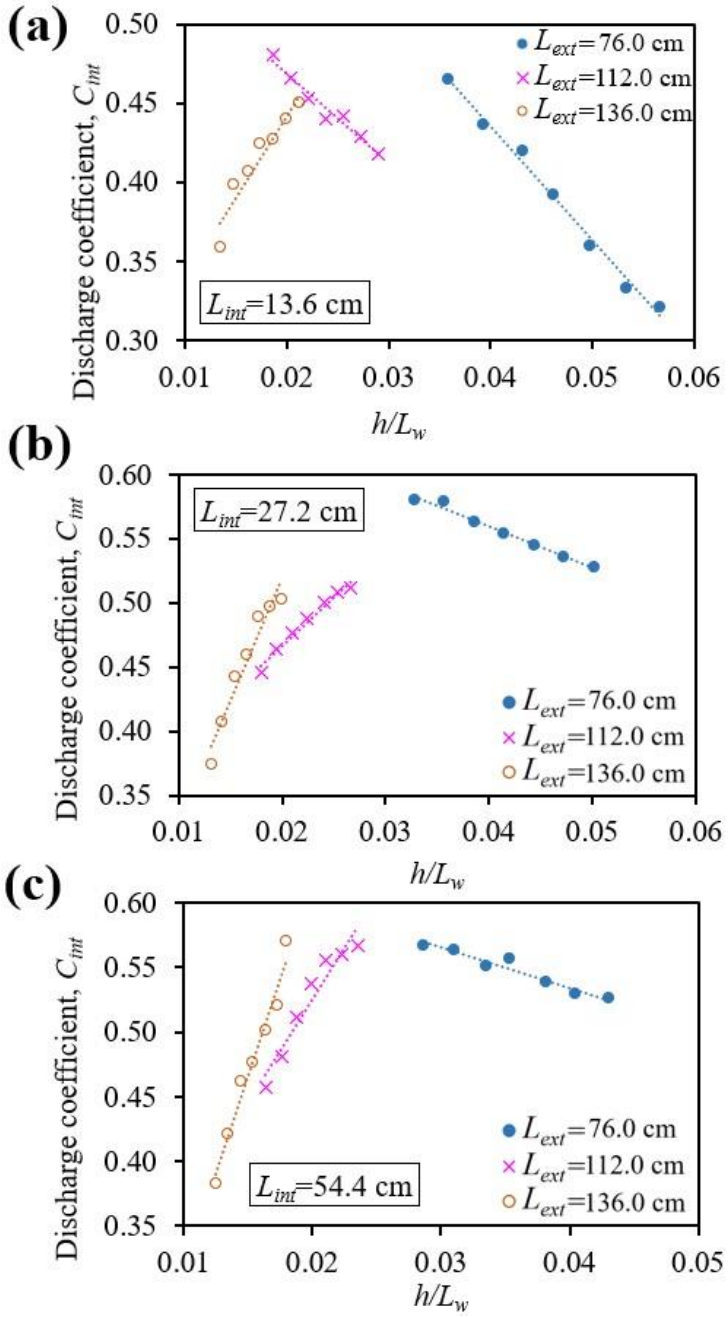

Figure 10. Variations in the discharge coefficient of internal weirs (Cint) versus h/Lext, in MHSs with external weir lengths of (a) 13.6 cm, (b) 27.2 cm, and (c) 54.4 cm. Dotted lines represent the fitted linear regression models

Table 6. Linear regression relationships between h/L_{ext} and the discharge coefficient in MHSs (C_{int}) for various internal and external weir lengths

Internal weir length (Lint), cm	External weir length, (Lext), cm	Least-squares linear regression model	R^2
13.6	76.0	C_{int} = -7.2009(h/L_{ext}) + 0.7232	0.990
	112.0	C_{int} = -5.6551(h/L_{ext}) + 0.5817	0.962
	136.0	C_{int} = 10.4130(h/L_{ext}) + 0.2340	0.915
27.2	76.0	C_{int} = -3.2410(h/L_{ext}) + 0.6892	0.985
	112.0	C_{int} = 7.5760(h/L_{ext}) - 0.3151	0.978
	136.0	C_{int} = 19.1740(h/L_{ext}) + 0.1355	0.946
54.4	76.0	C_{int} = -3.1014(h/L_{ext}) - 0.6584	0.932
	112.0	C_{int} = 15.9200(h/L_{ext}) - 0.2070	0.931
	136.0	C_{int} = 30.5130(h/L_{ext}) + 0.0080	0.973

Figure 10a shows that for MHS models with the smallest internal weir length (L_{int} = 13.6 cm), increasing the water head over the spillways (h/L_{ext}) for the models with external weir lengths of 76.0 cm and 112.0 cm resulted in negative slopes. The slope was greater for the model with external weir length (L_{ext}) of 112.0 cm. This means that increasing water head above the spillway decreased the discharge coefficient in these MHSs. However, increasing the external weir length to 136.0 cm resulted in a positive regression slope (Figure 10a). Figures 10b and 10c show the same trend for fixed internal weir lengths of 27.2 and 54.4 cm, respectively. In these models, increasing external weir length increased the slope of C_{int} versus h/L_{ext} regression lines (Table 6), indicating enhanced discharge efficiencies at higher flowrates.

Figure 10 and Table 6 show that stepwise increasing of L_{int} (i.e. from 13.6 cm to 27. 2 cm and then to 54.4 cm) for all external weir lengths, increased the slope of the fitted linear regression models.

3.4.3 Effects of the h/p Ratio on the Discharge Coefficient of Internal Weirs

Figure 11 shows variations in the discharge coefficients of internal weirs (C_{int}) versus h/p, in MHSs with external weir lengths of 76.0, 112.0, and 136.0 cm, considering a distance of p = 95 cm from the reservoir's bed to the top of the internal weirs' walls in all experiments. Characteristics of linear regression models fitted to the data points in Figure 11 (dotted lines) are listed in Table 7.

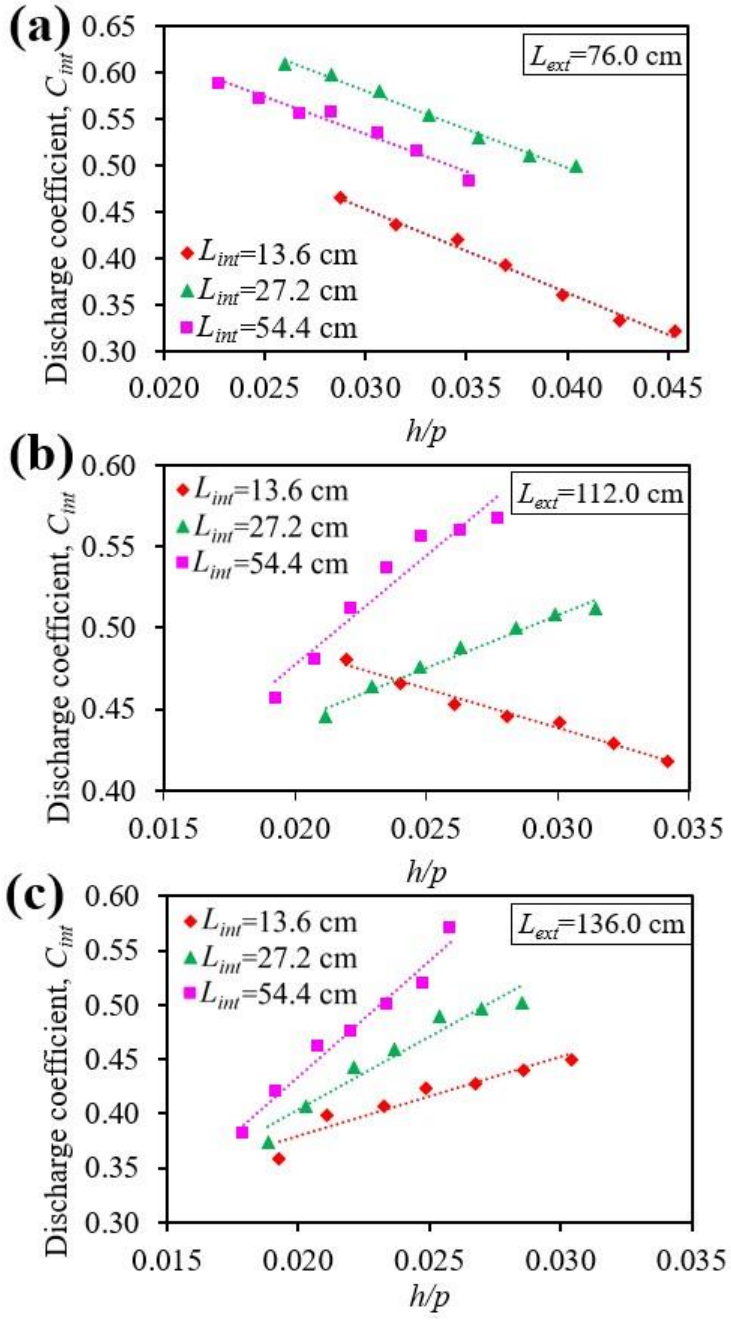

Figure 11. Variation of discharge coefficient in internal weirs (Cint) versus h/p, in MHSs with external weir lengths of (a) 76.0 cm, (b) 112.0 cm, and (c) 136.0 cm. Dotted lines represent the fitted linear regression models

Table 7. Linear regression relationships between *h/p* and the discharge coefficient in MHSs (Cint) for different internal and external weir lengths

External weir length (Lext), cm	Internal weir length (Lint), cm	Least-squares linear regression model	R^2
76.0	13.6	C_{int} = -9.0011(h/p) + 0.7232	0.990
	27.2	C_{int} = -8.2486(h/p) + 0.8284	0.990
	54.4	C_{int} = -3.8768(h/p) + 0.6584	0.932
112.0	13.6	C_{int} = -4.7952(h/p) + 0.5825	0.980
	27.2	C_{int} = 6.4261(h/p) - 0.3151	0.978
	54.4	C_{int} = 13.504(h/p) + 0.9306	0.931
136.0	13.6	C_{int} = 7.2741(h/p) - 0.2340	0.915
	27.2	C_{int} = 13.3930(h/p) - 0.1355	0.946
	54.4	C_{int} = 21.3150(h/p) + 0.0080	0.973

In general, the efficiency of the internal weirs is related to the flowrate passing through them. As mentioned, the use of a small external weir length of L_{ext} = 76.0 cm increased the fraction of the flowrate passing through the internal weirs in MHSs. In Figure 11a, the negative slope for C_{int} versus *h/p* could indicate bottlenecking in the internal weirs. Increasing the slope of the regression models in Table 7 from negative to positive when using greater sizes of L_{ext} and L_{int} indicates the capability of longer internal weirs to convey higher flowrates. Although adopting longer L_{ext} and L_{int} could resolve the issue of bottlenecking and produced positive slopes in Figures 11b and 11c (and Table 7), in order to utilize the full capacity of the internal weirs and thus obtaining higher discharge coefficients, higher flowrates or higher values of *h/p* were also required. This indicates that in order to obtain a high discharge coefficient in an MHS model, geometric design of the spillway needs to be optimized.

3.5. Economical Design of Classical and Modified Horseshoe Spillways

As discussed, variations in the water head as well as the internal and external weirs lengths affected the discharge efficiency of CHSs and MHSs. Dimensional analysis showed that the length of external weirs in MHSs affected the fraction of the flowrate passing through the internal weirs. Therefore, the proportion of the internal weir length to the external weir length is a key factor in controlling bottlenecking in internal weirs. Figures 12 and 13 represent the three-dimensional surface and contour plots of reduced cubic models fitted to the data points obtained from the experiments conducted on CHS and MHS models, respectively.

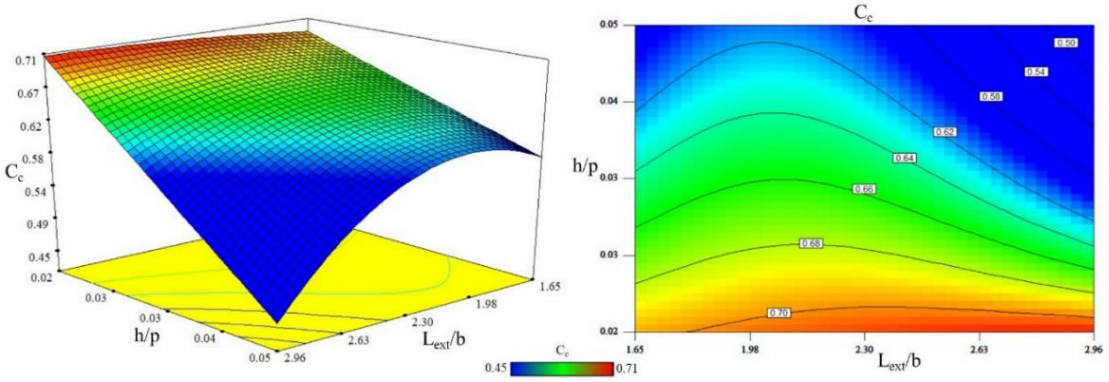

Figure 12. 3D surface and contour plots for the effects of h/p and Lext/b on the discharge coefficient in CHSs

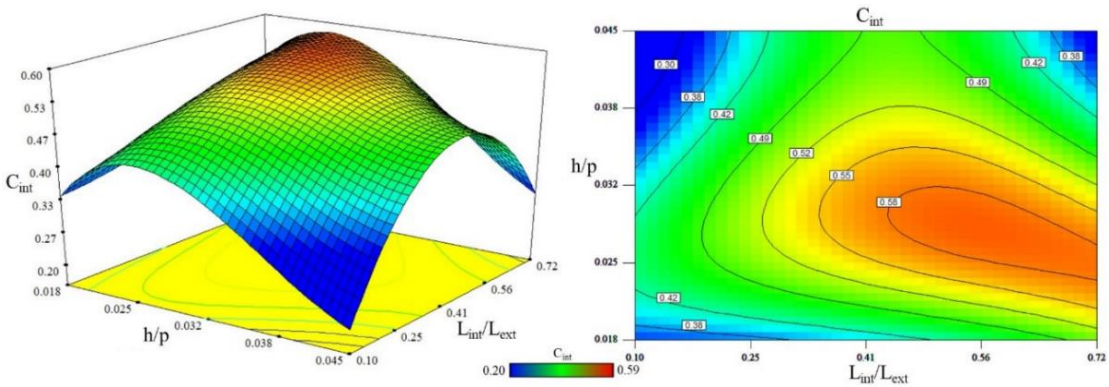

Figure 13. 3D surface and contour plots for the effects of h/p and Lint/Lext on the discharge coefficient in MHSs

ANOVA was performed to evaluate the significance of h/p and L_{ext}/b factors as independent variables and their interactions on the discharge coefficient in CHSs. Similarly, for MHSs, ANOVA was performed considering h/p and L_{int}/L_{ext} as independent variables. Results are presented in Tables 8 and 9 for CHSs and MHSs, respectively. All variables' interactions that were statistically non-significant (p-value > 0.05)–i.e. $(h/p)^2$, $(L_{ext}/b)(h/p)^2$, $(L_{ext}/b)^3$, and $(h/p)^3$ for CHSs, and $(h/p)^2$ (L_{int}/L_{ext}) and $(L_{int}/L_{ext})^3$ for MHSs–were excluded from the cubic models.

Table 8. Analysis of variance for the reduced cubic model fitted to the experimental results of CHSs

Source	Sum of squares	Degrees of freedom	Mean square	F-value	p-value
Model	0.032	5	6.388×10-3	85.82	< 0.0001
L_{ext}/b	4.119×10-3	1	4.119×10-3	55.34	< 0.0001
h/p	6.162×10-3	1	6.162×10-3	82.79	< 0.0001
$(L_{ext}/b)\times(h/p)$	1.866×10-3	1	1.866×10-3	25.07	< 0.0001
$(L_{ext}/b)^2$	3.765×10-3	1	3.765×10-3	50.58	< 0.0001
$(L_{ext}/b)^2\times(h/p)$	1.080×10-3	1	1.080×10-3	14.51	0.0005
Residual	2.679×10-3	36	7.443×10-5	-	-
Total	0.035	41	-	-	-
$\boldsymbol{R^2}$	0.923	-	-	-	-
Adjusted $\boldsymbol{R^2}$	0.912	-	-	-	-

Table 9. Analysis of variance for the reduced cubic model fitted to the experimental results of MHSs

Source	Sum of squares	Degrees of freedom	Mean square	F-value	p-value
Model	0.51	7	0.073	163.80	< 0.0001
h/p	0.024	1	0.024	54.98	< 0.0001
L_{int}/L_{ext}	0.081	1	0.081	182.45	< 0.0001
$(h/p)\times(L_{int}/L_{ext})$	0.025	1	0.025	55.16	< 0.0001
$(h/p)^2$	0.066	1	0.066	148.98	< 0.0001
$(L_{int}/L_{ext})^2$	0.082	1	0.025	185.00	< 0.0001
$(h/p)\times(L_{int}/L_{ext})^2$	0.025	1	0.025	55.37	< 0.0001
$(h/p)^3$	0.015	1	0.015	33.94	< 0.0001
Residual	0.052	118	4.448×10-4	-	-
Total	0.56	125	-	-	-
$\boldsymbol{R^2}$	0.908	-	-	-	-
Adjusted $\boldsymbol{R^2}$	0.901	-	-	-	-

According to Tables 8 and 9, the models' p values of < 0.0001 indicate that the retained independent variables could explain a significant proportion of the variance and show that the fitted reduced cubic models were statically significant. In addition, high values of R^2 and adjusted R^2 for both the reduced cubic models confirmed the accuracy of these models to describe experimental results.

The least-squares relationship between discharge coefficients in CHSs and MHSs in the reduced cubic models are shown in Equations 14 and 15, respectively.

$$C_c = 1.1377 - 0.4017(L_{ext}/b) - 25.7294(h/p) + 22.9984(L_{ext}/b)(h/p) + 0.1065(L_{ext}/b)^2 - 5.8264(L_{ext}/b)^2(h/p) \quad (6)$$

$$C_{int} = -0.9215 + 132.9068(h/p) - 1.3361(L_{int}/L_{ext}) + 77.2904(h/p)(L_{int}/L_{ext}) - 4153.5448(h/p)^2 + 2.0198(L_{int}/L_{ext})^2 - 98.8135(h/p)(L_{int}/L_{ext})^2 + 36963.5881(h/p)^3 \quad (7)$$

From an economical point of view, the goal is to design spillways with the highest discharge efficiencies while adopting the minimum sizes of internal and external weirs, in order to reduce the construction costs. As seen from Figure 12, higher discharge coefficients in CHSs occurred for low h/p values. For $h/p < 0.03$, increasing the weir length could not significantly increase the discharge coefficient. In higher h/p values ($h/p > 0.04$), increasing the weir length to L_{ext}/b=2.1 increased the discharge coefficient; however, longer weir lengths resulted in decreased efficiency of CHSs.

For internal weirs in MHSs, adopting very low and very high ratios of L_{int}/L_{ext} decreased efficiencies of the internal weirs. In addition, h/p ratio significantly affected the efficiency of internal weirs. It was shown that variations in the water head and sizes of internal and external weirs caused significant changes in the hydraulic behaviour of flow passing

through the internal weirs. This reflected in the high interactions between h/p and L_{int}/L_{ext}, as shown in Table 9. As Figure 13 shows, higher efficiencies for the internal weirs occurred for rather high ratios of L_{int}/L_{ext} ($L_{int}/L_{ext} > 0.50$) and low h/p values ($0.2 < h/p < 0.3$).

As a conclusion, using small external weir lengths in MHSs would reduce construction costs and still could result in acceptable discharge efficiencies in the external weirs. Adopting a L_{int}/L_{ext} ratio between 0.5 to 0.6 would result in high discharge coefficients in internal weirs. Using higher ratios of L_{int}/L_{ext} could reduce h/p and increase efficiencies in both the internal and external weirs.

4. Conclusion

Results of this study showed that compared to a rectangular weir, an increased weir length in a CHS could reduce the water head more efficiently and increase the spillway's discharge efficiency. For high flowrates or high h/p values, increasing the weir length could enhance the discharge efficiency of CHSs.

Incorporating an internal weir in a CHS to create an MHS not only could improve the overall efficiency of the spillway and allow it to convey more flow of water, but also could reduce water head over the spillway. In turn, reduced water head (i.e., reduced h/p) resulted in increased efficiencies of both the internal and external weirs. Incorporating an internal weir could also eliminate the formation of rooster-tail hydraulic jump in a CHS, increasing the durability of the spillway.

The relative size of the internal weir compared to the length of the external weir (L_{int}/L_{ext}) was found to be a key parameter in design of MHSs. Increasing the size of external weirs in MHSs increased the discharge overflowing the external weirs and, consequently, decreased the discharge flowing through the internal weirs. Hence, adopting a short external weir could increase the fraction of discharge flowing through the internal weirs. In addition, increasing the size of the internal weir could resolve issues of bottlenecking in the internal weir and allowed the length of the external weir to be decreased. Experimental results showed that the highest discharge efficiencies in MHSs occurred for low h/p and high L_{int}/L_{ext} values.

This study mainly investigated the hydraulic characteristic of classical and modified horseshoe spillways. Further experiments are recommended to investigate energy dissipation as well as the effects of other parameters on efficiencies for both classical and modified horseshoe spillways. This can include (1) the effects of size and height of an end sill on energy dissipation and the efficiency of spillways, (2) the effects of flowrate on the height and length of rooster-tail jumps in classical horseshoe spillways, and (3) the effects of the internal weir's height on submergence, efficiency, and energy dissipation in modified horseshoe spillways.

5. Acknowledgements

Experiments of this study were carried out in the Hydraulics Laboratory of the Water Engineering Department, University of Tabriz. Thanks also go to Julie Longo, technical writer for UNLV's Howard R. Hughes College of Engineering for editorial review.

6. Conflicts of Interest

The authors declare no conflict of interest.

7. References

[1] U. S. Bureau of Reclamation, Design of small dams, 1987. https://www.usbr.gov/tsc/techreferences/mands/mands-pdfs/SmallDams.pdf.

[2] Falvey, Henry T. "Hydraulic Design of Labyrinth Weirs" (November 18, 2002). doi:10.1061/9780784406311.

[3] Dabling, M. R., and B. P. Tullis. "Labyrinth Weirs with Angled Approach Flow." Journal of Hydraulic Engineering 144, no. 12 (December 2018): 06018014. doi:10.1061/(asce)hy.1943-7900.0001544.

[4] Vischer, Daniel L., and Willi H. Hager. "Dam hydraulics." John Wiley & Sons, Chichester, West Sussex PO 19 1 UD(UK). 316 (1998): 316.

[5] Carollo, Francesco Giuseppe, Vito Ferro, and Vincenzo Pampalone. "Testing the Outflow Process over a Triangular Labyrinth Weir." Journal of Irrigation and Drainage Engineering 143, no. 8 (August 2017): 06017007. doi:10.1061/(asce)ir.1943-4774.0001198.

[6] Khatsuria, R. M. "Hydraulics of Spillways and Energy Dissipators" (October 27, 2004). doi:10.1201/9780203996980.

[7] Mays, Larry W., ed. Hydraulic design handbook. McGraw-Hill Professional Publishing, 1999.

[8] Tullis, Blake P., J. Chandler Young, and M. A. Chandler. "Head-discharge relationships for submerged labyrinth weirs." Journal of Hydraulic Engineering 133, no. 3 (2007): 248-254. doi:10.1061/(ASCE)0733-9429(2007)133:3(248).

[9] B.M. Crookston, "Labyrinth weirs." Utah State University, 2010.

[10] Crookston, B. M., and B. P. Tullis. "Arced Labyrinth Weirs." Journal of Hydraulic Engineering 138, no. 6 (June 2012): 555–562. doi:10.1061/(asce)hy.1943-7900.0000553.

[11] Seamons, Tyler Robert. "Labyrinth weirs: A look into geometric variation and its effect on efficiency and design method predictions." (2014).

[12] Kaya, Nihat, M. Emin Emiroglu, and Hayrullah Agaccioglu. "Discharge Coefficient of a Semi-Elliptical Side Weir in Subcritical Flow." Flow Measurement and Instrumentation 22, no. 1 (March 2011): 25–32. doi:10.1016/j.flowmeasinst.2010.11.002.

[13] Tiwari, Harinarayan, and Nayan Sharma. "Developments to Improve Hydraulic Competence of Spillways." Aquatic Procedia 4 (2015): 841–846. doi:10.1016/j.aqpro.2015.02.105.

[14] Lapotre, Mathieu G. A., and Michael P. Lamb. "Hydraulics of Floods Upstream of Horseshoe Canyons and Waterfalls." Journal of Geophysical Research: Earth Surface 120, no. 7 (July 2015): 1227–1250. doi:10.1002/2014jf003412.

[15] Akan, A. Osman. "Hydraulic Structures." Open Channel Hydraulics (2006): 200–265. doi:10.1016/b978-075066857-6/50007-2.

[16] Marriott, Martin. Nalluri and Featherstone's, "Civil Engineering Hydraulics: Essential Theory with Worked Examples.", John Wiley & Sons, 2016.

[17] Hong, Seung Ho, Terry W. Sturm, and Juan A. González-Castro. "Transitional Flow at Low-Head Ogee Spillway." Journal of Hydraulic Engineering 144, no. 2 (February 2018): 04017062. doi:10.1061/(asce)hy.1943-7900.0001398.

[18] Leite Ribeiro, M., M. Bieri, J.-L. Boillat, A. J. Schleiss, G. Singhal, and N. Sharma. "Discharge Capacity of Piano Key Weirs." Journal of Hydraulic Engineering 138, no. 2 (February 2012): 199–203. doi:10.1061/(asce)hy.1943-7900.0000490.

[19] Saadatnejadgharahassanlou, Hamid, Amin Gharehbaghi, Saeid Mehdizadeh, Birol Kaya, and Javad Behmanesh. "Experimental Investigation of Discharge Coefficient over Novel Kind of Sharp-Crested V-Notch Weir." Flow Measurement and Instrumentation 54 (April 2017): 236–242. doi:10.1016/j.flowmeasinst.2017.02.008.